Nanoscale

Accepted Manuscript

This article can be cited before page numbers have been issued, to do this please use: L. Chang, X. He, L. Chen and Y. Zhang, *Nanoscale*, 2017, DOI: 10.1039/C6NR09944K.

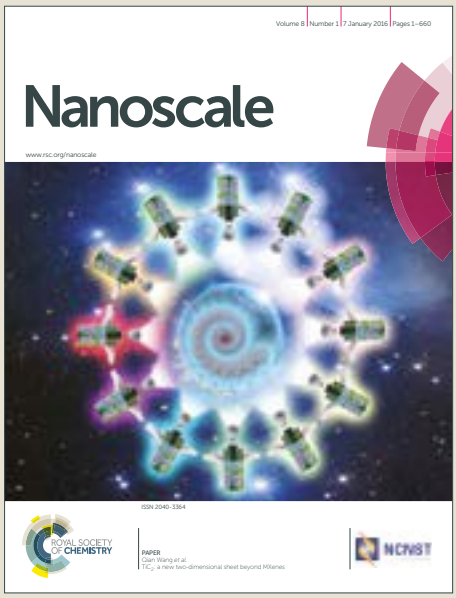

ROYAL SOCIETY OF CHEMISTRY

rsc.li/nanoscale

View Article Online
DOI: 10.1039/C6NR09944K

Journal Name

ARTICLE

Received 00th January 20xx,
Accepted 00th January 20xx

DOI: 10.1039/x0xx00000x

www.rsc.org/

A novel fluorescent turn-on biosensor based on QDs@GSH-GO fluorescence resonance energy transfer for sensitive glutathione *S*-transferases sensing and cellular imaging

Lifang Chang[a], Xiwen He[a], Langxing Chen,*[a,b] and Yukui Zhang[a,c]

A novel fluorescent turn-on biosensor based on fluorescence resonance energy transfer (FRET) from the GSH functionalized Mn-doped ZnS QDs to graphene oxide (GO) was constructed to determine the glutathione *S*-transferases (GSTs) in live cell and human urine. The QDs@GSH is absorbed on GO surface via hydrogen bonding interaction between the GSH on the surface of QDs@GSH and GO, as a result, the fluorescence quenching of the QDs@GSH takes place because of FRET. The FRET efficiency from QDs@GSH to GO was calculated to be 86.3%. However, in the presence of GSTs, the FRET process could be inhibited by the specific interaction between the GSH on the surface of QDs@GSH and GSTs, which would keep the QDs@GSH far away from the GO surface, leading to the recovery of the fluorescence. The proposed sensor exhibited high sensitivity, selectivity, and excellent specificity in the buffer, live cells and human urine for the detection of GSTs. Under the physiological conditions (pH 7.4), dissociation constants and the detection limit of GST and ATP6V1F (a GST-tagged protein) were estimated to be 8.0×10^{-9} M, 2.1×10^{-10} M and 3.5×10^{-9} M, 7.2×10^{-11} M, respectively. The presented method has been successfully utilized for the determination of the GSTs in live cells and human urine without any complicated pretreatment and the recovery was in the range of 80%-90%.

Introduction

Glutathione *S*-transferases (GSTs) are a large family of ubiquitous detoxification enzymes in organisms, which can protect tissues from the toxic chemicals by catalyzing the coordination of the tripeptide glutathione (GSH) to the electrophilic organic compounds such as endogenous superoxide radicals and toxic metabolites.[1-3] GSTs also often exhibit a highly overexpressed in certain tumor cells compared with the corresponding normal tissues, and they play a significant role in the development of resistance to chemotherapeutic agents because they detoxify these compounds.[4-6] Consequently, there is a need of sensitively detecting the GSTs. Besides, GSTs are widely applied to tag the fusion proteins to selectively separate proteins from proteomic analysis due to their specificity to GSH.[7,8] Currently, the conventional methods for GSTs quantitative assay are high-performance liquid chromatography (HPLC),[9-11] mass spectrometry (MS),[12-14] electrochemical sensors,[15] bioluminescent sensors,[16,17] sodium dodecyl sulfate polyacrylamide gel electrophoresis (SDS/PAGE),[18,19] static light scattering (SLS)[20] and fluorescent sensor.[21-25] Among them, fluorescent methods are thought to be potential for the development of highly sensitive and relatively simple analysis protocols. In recent years, fluorescence sensors based on GSH functionalized gold nanoparticles (AuNPs),[26] gold nanoclusters (AuNCs)[21,25] and quantum dot (QDs)[17,22] with their high surface-to-volume ratio, are widely used as effective affinity probes to capture and analyze target GST or GST-tagged proteins.

Nowadays, the fluorescence resonance energy transfer (FRET) between emerging nanomaterials and biomolecular recognition units has attracted on considerable research effects on the development of novel biosensing and diagnostic techniques.[27,28] Recently, QDs-FRET system has emerged as a powerful tool in the detection of ions,[29] organic small molecules[30] or biomacromolecules[25,31-34] (proteins and nucleic acids). QDs has been widely used as the energy donors due to their high fluorescence quantum yields, high stability against degradation and photobleaching, broad absorption, narrow emission and size-controlled emission, while organic dyes,[33,35,36] AuNPs[32,37], graphene and graphene oxide (GO)[38-42] are used to the energy acceptors. Compared with the organic dyes and AuNPs, GO are regarded as the advanced acceptors due to their high efficiency of energy-transfer and electron transfer.[43,44] The theoretical calculations confirmed that graphene can be excellent fluorescence quencher with the long range absorption, which is helpful for realizing sensitive fluorescence sensing on graphene-FRET sensors.

[a] *Research Center for Analytical Sciences, College of Chemistry, Tianjin Key Laboratory of Biosensing and Molecular Recognition, State Key Laboratory of Medicinal Chemical Biology, Nankai University, Tianjin 300071, China. Tel: +86-0-22-23502458; E-mail: lxchen@nankai.edu.cn.*
[b] *Collaborative Innovation Center of Chemical Science and Engineering (Tianjin), Tianjin 300071, China.*
[c] *Dalian Institute of Chemical Physics, Chinese Academy of Sciences, Dalian, 116023, China.*
†Electronic Supplementary Information (ESI) available. See DOI: 10.1039/x0xx00000x

Among the reported QDs-FRET biosensors, the CdS, CdSe, CdS/CdSe, CdTe QDs as donors have been developed. However, QDs containing of Cd^{2+} can exert genotoxic, epigenetic, and metalloestrogenic effects in cells,[45] and the self-quenching fluorescence induced by energy transfer between adjacent QDs or intramolecular ground-state dimer complex which may confine their applications in bioanalysis.[46] The metal ions doped QDs not only potentially retain almost the above advantages of undoped QDs, but also avoid the self-quenching problem, and are thus regarded as a new class of luminescent materials. Therefore, doped QDs as energy donors in FRET systems are attractive for sensing application.[47-51] The metal ions doped ZnS and ZnO QDs have longer dopant emission lifetime and potentially lower cytotoxicity in comparison with typical CdSe and CdTe QDs. This property makes the doped QDs as excellent donors of FRET for applications of *in vivo* and *in vitro* chemo/biosensing and bioimaging.[46,52] It is expected that the highly absorptive nanomaterials such as graphene oxide, AuNPs and Au nanorods as energy acceptors in FRET with Mn-doped QDs will generate novel sensing platforms.

Previously, our group had developed a fluorescent biosensor for GST detection based on FRET between GSH modified Au nanoclusters (AuNCs@GSH), as an energy donor, and amine-terminated Au nanoroads (AuNRs), as an energy acceptor.[25] Inspired by this observation, herein we have designed a novel turn-on fluorescence biosensor based on FRET from GSH-functionalized Mn-doped ZnS QDs (QDs@GSH) to graphene oxide (GO), a highly efficient energy transfer acceptor, for the determination of GSTs (Scheme 1). QDs@GSH can absorb on GO surface via hydrogen bonding interaction between the GSH on the surface of QDs and GO. The fluorescence of the QDs would be sufficiently quenched with the efficient energy transfer process from QDs to GO. However, when adding GSTs, GSH preferred to combine GSTs with the specific interaction between GSH and GST which further replaced the interaction between GSH and GO, resulting in QDs being kept away from the GO surface, the FRET process being inhibited, fluorescence quenching decreasing and the fluorescence recovering. Herein, GST (from horse liver) and ATP6V1F (a GST-tagged protein from human) as the model of GSTs were introduced to the FRET system in the subsequent assays.

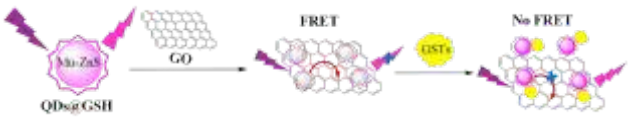

Scheme 1 Schematic illustration of GSTs detection based on QDs@GSH-GO FRET sensing system.

Experimental section

Reagents and materials

Glutathione *S*-transferase (GST), ATP6V1F (a GST-tagged protein), bovine serum albumin (BSA), cytochrome C (Cyt), bovine hemoglobin (BHb), immunoglobulin G (IgG), lysosome (Lyz), and transferrin (Trf) were purchased from Sigma-Aldrich (USA). Znic sulfate hepahydrate ($ZnSO_4·7H_2O$), manganese sulfate tetrahydrate ($MnSO_4·4H_2O$), sodium sulfide nonahydrate ($NaS·9H_2O$), sodium chloride (NaCl), magnesium chloride ($MgCl_2$), calcium chloride ($CaCl_2$), potassium chloride (KCl), cadmium chloride ($CdCl_2$), cobalt chloride ($CoCl_2$), nickel(II) chloride ($NiCl_2$), iron(III) chloride ($FeCl_3$), copper(II) chloride ($CuCl_2$) and zinc chloride ($ZnCl_2$) were all obtained from Tianjin Chemical Reagent Company (Tianjin, China), and used directly without further purification. Glutathione (GSH) was purchased from J&K Chemical (Beijing, China). Graphene oxide (GO) was purchased from XFNANO (Nanjing, China). Other reagents were of analytical grade or better. Deionized water was prepared with an Aquapro ultrapure water system (Chongqing, China).

Instruments

The crystal structure of the NPs was determined by an X-ray diffractometer (XRD). The XRD pattern of the sample was recorded with a Shimadzu (Japan) D/Max-2500 diffractometer, using a monochromatized X-ray beam with nickel-filtered Cu Kα radiation. The XRD patterns were collected in the range of $3^o < 2\theta < 80^o$ with a dwelling time of 2 s and a scan rate of 6.0^o min^{-1}. The size and morphology of the NPs were measured by a JEOL JEM-2100 transmission electron microscope (TEM). The graphene oxide, QDs and QDs-GO dispersed in deionized water were cast onto a carbon-coated copper grid sample holder followed by evaporation at room temperature. Fourier transform infrared (FT-IR) spectra (4000-400 cm^{-1}) in KBr were recorded using the AVATAR 360 FT-IR spectrophotometer (Nicolet, Waltham, USA). The fluorescence responses to GSTs with the prepared QDs-GO system were obtained by using a FL-4500 spectrophotometer (Shimadzu, Japan). The fluorescent images of living cells were observed under an inversion fluorescence microscope (Nikon, Japan).

Synthesis of GSH modified Mn-doped ZnS QDs

The synthetic routes of GSH-Mn-doped ZnS QDs are modified according to the literature previously.[53] $ZnSO_4·7H_2O$ (1.8 g, 6.25 mmol), $MnSO_4·4H_2O$ (0.11 g, 0.5 mmol) was dissolved in 20 mL ultrapure water in 100 mL three-necked flask, stirred under argon at room temperature for 10 min, and then added 10 mL aqueous solution containing $Na_2S·9H_2O$ (1.5 g, 6.25 mmol). After stirring for 30 min, 10 mL ultrapure water containing of GSH (1.92 g, 6.25 mmol) was added into the solution and then kept stirring for 20 h. Finally, the product was precipitated with absolute ethanol, separated by centrifuging, washed with ultrapure water and absolute ethanol for three times, and dried at 30 ^oC in vacuum for 3 h.

Procedures for determining GSTs based on QDs@GSH-GO

For the determination of GST and ATP6V1F, the certain concentrations of GSH-Mn-doped ZnS QDs (final concentration of 50 mg L^{-1}) and GO (final concentration of 240 mg L^{-1}) were mixed and incubated for 1 h in 10 mM PBS buffer (pH 7.4), and then various concentrations of GST and ATP6V1F were added to the mixture and further incubated for 2 h, respectively. The fluorescence spectra of the final mixture were also measured using the FL-4500 spectrophotometer.

Selectivity of QDs@GSH-GO for sensing GSTs

GST, ATP6V1F, BSA, Cyt, BHb, IgG, Lyz, and Trf were selected to evaluate the selectivity of the QDs@GSH-GO system. Each of the QDs@GSH-GO solutions (200 μL 50 mg L^{-1}) in 2 mL tubes, containing GST (100.0 nM) or ATP6V1F (10.0 nM) or each of six proteins (1.0 μM), were incubated for 2 h at room temperature, and then characterized by fluorescent method. The response to the GSTs and the analogues with QDs-GO system were compared.

The metal ions (Ca^{2+}, Cd^{2+}, Co^{2+}, Cu^{2+}, Fe^{3+}, K^{+}, Mg^{2+}, Na^{+}, Ni^{2+}, Zn^{2+}) with concentration of 1 μM were added into the QDs@GSH-GO solutions in the presence of 100.0 nM GST or 10.0 nM ATP6V1F, and then incubated for 2 h at room temperature, respectively. Competition events were also monitored by fluorescent spectra, and all tests were conducted in triplicate.

Determination of GSTs in urine samples

Urine sample from a healthy volunteer was selected for spiked sample analysis. First, 1 μL urine sample was diluted 100 times with 10 mM phosphate buffer (PBS, pH = 7.4) containing of QDs@GSH-GO system. Then 0.0-1.0 nM standard solutions of ATP6V1F were added to 1 mL of diluted urine sample solution in 2 mL plastic tubes, respectively. The tubes were shaken on a rotator for 2 h at room temperature. Finally, the fluorescence spectra of solutions were directly measured.

Fluorescence imaging of GSTs in living cells

The living L929 cells were cultured in the Dulbecco's modified eagle media (DMEM) and 10% fatal bovine serum (FBS) medium to get a suitable density. The cells were spiked with ATP6V1F (final concentration of 1.0 nM) and incubated for 30 min at 37 ^{o}C, and then washed with 10 mM PBS (pH = 7.4) three times. The fluorescent imaging experiments for intracellular GSTs were conducted with L929 cells, treated with the QDs@GSH-GO system for 30 min at 37 ^{o}C. The excited wavelength of the laser was 330-370 nm in ultraviolet region. The fluorescence for the single cell was analyzed by inversion fluorescence microscope.

Results and discussion

Characterization of QDs@GSH-GO FRET system

The as-prepared GSH modified Mn-dopped ZnS QDs and QDs@GSH-GO system were characterized by TEM, XRD and FT-IR. The Fig.1A revealed the formation of monodisperse GSH-capped Mn-doped ZnS QDs with spherical shape possessing a diameter of approximately 3.5 nm. The particle hydrodynamic size analyzer (Fig. S1A, Electronic Supplementary Information) shows that determined particle sizes of QDs@GSH are close to those measured by TEM. The QDs@GSH displayed the narrow particle size distribution and the Zeta potential of -18 mV (Fig. S1B, Electronic Supplementary Information). The GO had layered structure, and the surface of the sheet was relatively smooth (Fig. 1B). The TEM image of QDs@GSH-GO is shown in Fig. 1C. Obviously, a large quantity of uniform spherical QDs@GSH

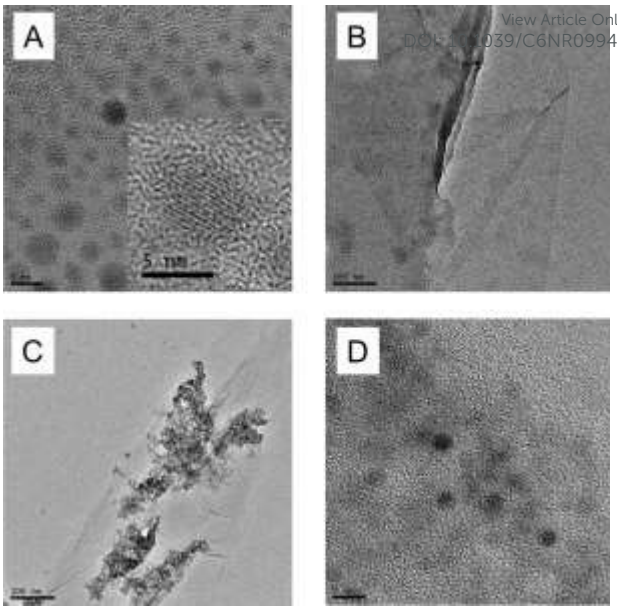

Fig. 1 HRTEM images of QDs@GSH (A), TEM images of GO (B), QDs@GSH-GO (C) and HRTEM images of QDs@GSH-GO (D).

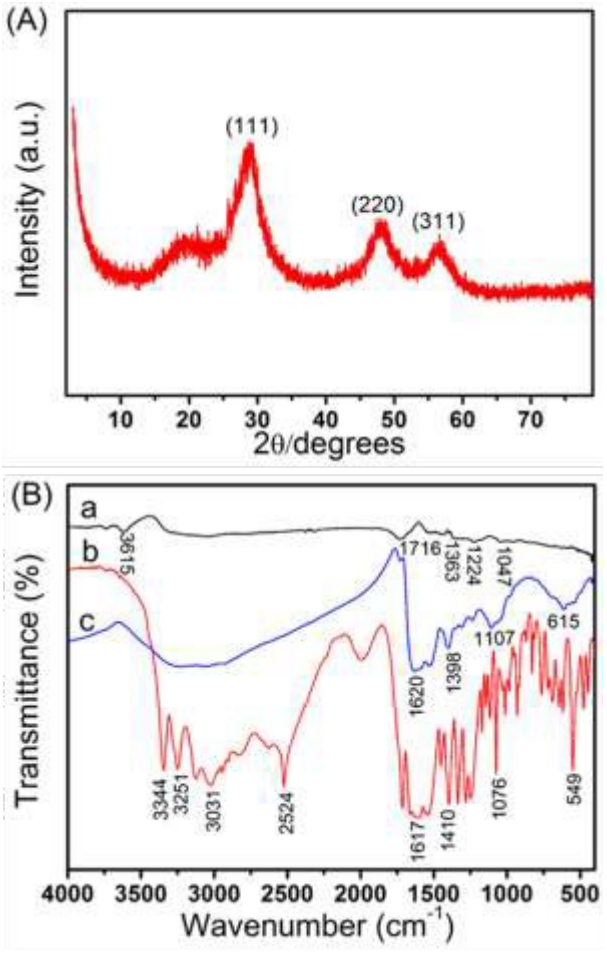

Fig. 2 (A) XRD pattern of the QDs@GSH and (B) FT-IR spectra of GO (curve a), GSH (curve b) and QDs@GSH (curve c).

absorbed on the surface of GO. In addition, the HRTEM images of QDs@GSH-GO show the two-dimensional GO sheet is well decorated by a large quantity of spherical GSH-Mn-ZnS QDs particles (with average size of about 3.5 nm) and the lattice was clearly visible. This result revealed that QDs@GSH-GO system had been constructed successfully compared with GO alone in Fig. 1B.

The XRD pattern of Mn-doped ZnS QDs exhibits a cubic zinc sulfide crystal structure with peaks for (111), (220), and (311) planes (Fig. 2A). It is suggested that the crystalline lattices of Mn-doped ZnS QDs are pretty integrated. FT-IR spectra of GO, GSH and QDs@GSH are shown in Fig. 2B, respectively. As for GO, the strong and wide band at 3615 cm^{-1} is O-H stretching vibration, the peaks at 1716, 1363, 1244 and 1047 cm^{-1} are attributed to C=O, O-H deformation vibration, C-OH and C-O stretching vibration, respectively. For GSH, 2524 cm^{-1} is S-H stretching vibration band, 1617 cm^{-1} is N-H bending vibration band, 1410 cm^{-1} is C-N stretching vibration band. Concerning the QDs@GSH, 615 cm^{-1} is the characteristic vibration band of Zn-S, and the disappearance of 2524 cm^{-1} in Fig. 2B (c) revealed that the GSH had also been functionalized on the surface of the Mn-doped ZnS QDs successfully.

FRET between QDs@GSH and GO

As shown in Fig. 3A, the fluorescence emission bands of the prepared QDs are at the wavelength of 450 nm (ZnS QDs) and 607 nm (Mn-doped ZnS QDs), respectively. The two fluorescence emission peaks of QDs were largely overlapped with the absorption spectrum of GO, which indicated that they were likely a nice pair of FRET donor/acceptor, which met exactly the condition of FRET. The absolute quantum yield of the GSH modified Mn-doped ZnS QDs was measured to be 49.6%. The strong fluorescence of QDs@GSH was efficiently quenched about 86.3% after incubation with GO in Fig. 3B. This conclusion could be confirmed by the obvious changes of fluorescence lifetimes from 1.87 ns for QDs@GSH to 1.38 ns for QDs@GSH-GO after addition of GO (Fig. S2, Electronic Supplementary Information). The lifetimes of QDs and QDs-GO FRET system are shown in Table S1 (Electronic Supplementary Information). The significant fluorescence quenching of QDs@GSH was mainly attributed to the hydrogen bonding interaction between -COOH or NH_2 groups of the GSH on the surface of QDs and -OH or COOH groups of GO leading to the energy transfer from QDs to GO. The addition of GST leads to the fluorescence recovery due to the formation of GSH-GST complexes which keep the QDs away from GO surface. The distance between QDs@GSH and GO was calculated to be ~3.8 nm according to the size of QDs@GSH and hydrogen bond length, which met the occurrence of FRET. A similar work has been reported for FRET system based on ssDNA-functionalized CdTe QDs and GO.[42] The fluorescence quenching of QDs was induced by QDs absorbing on GO surface via the π-π stacking interaction between the GO and the base, and hydrogen bonding interaction between nitrogen/oxygen containing groups on the ssDNA and while specific interaction between the introduced target DNA and the ssDNA resulted in the distance increase between the QDs, which significantly hindered the FRET and, thus the fluorescence of QDs was recovered. In comparison with the above CdTe QDs-GO FRET using the toxic metal ions, the Mn-doped ZnS QDs made from less-harmful elements was selected to fabricate a turn-on FRET biosensor for the detection of the GSTs in complex biological samples.

The relation between the fluorescent quenching effect on the QDs@GSH and the amount of GO was also studied. The fluorescence intensity of QDs@GSH gradually decreased with the increase of GO concentrations (Fig. 3C), and the quenching efficiency achieved a plateau when the amounts of GO were more than 0.24 mg mL^{-1} (Fig. 3D). The calculated quenching efficiency or FRET efficiency is defined as:

$$E = 1 - \frac{F_{DA}}{F_D} \qquad (1)$$

Where F_{DA} and F_D are the fluorescent intensities of the donor in the presence and absence of the acceptor. As a result, 0.24 mg mL^{-1} was selected as the final concentration of GO for the subsequent experiments. The effect of reaction time on the quenching is also investigated. It is exhibited that the fluorescence of the QDs@GSH was sufficiently quenched within 60 min in the presence of GO (Fig. S3, Electronic

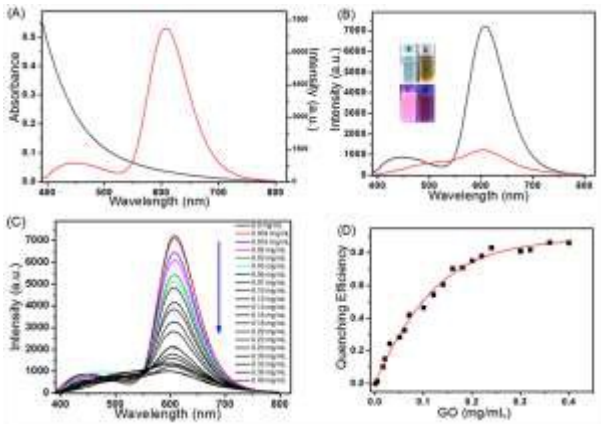

Fig. 3 (A) Fluorescence emission of the QDs@GSH (red curve), and the absorption spectrum of GO (black curve). (B) Fluorescence emission of QDs@GSH before (black curve) and after (red curve) incubation with GO. (The inset shows a photograph of the QDs@GSH and QDs@GSH-GO in 10 mM PBS (pH = 7.4) under ambient light (a, b) and irradiated by 285 nm light (c, d).) (C) Fluorescence spectra of the QDs@GSH after adding into the different concentrations of GO. (D) Plot of fluorescence quenching efficiency versus GO concentration.

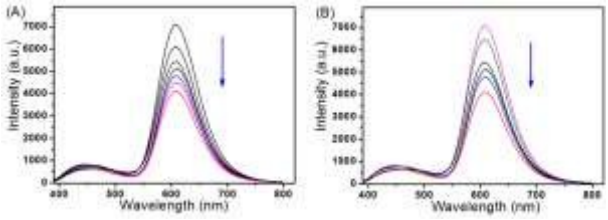

Fig. 4 Fluorescence emission spectra of the QDs@GSH (50 mg L^{-1}) in the presence of various concentrations (0.0, 1.0, 5.0, 10.0, 30.0, 50.0, 100.0 nM) of GST (A) and (0.0, 1.0, 3.0, 5.0, 8.0, 10.0 nM) of ATP6V1F (B) in 10 mM PBS (pH 7.4).

View Article Online
DOI: 10.1039/C6NR09944K

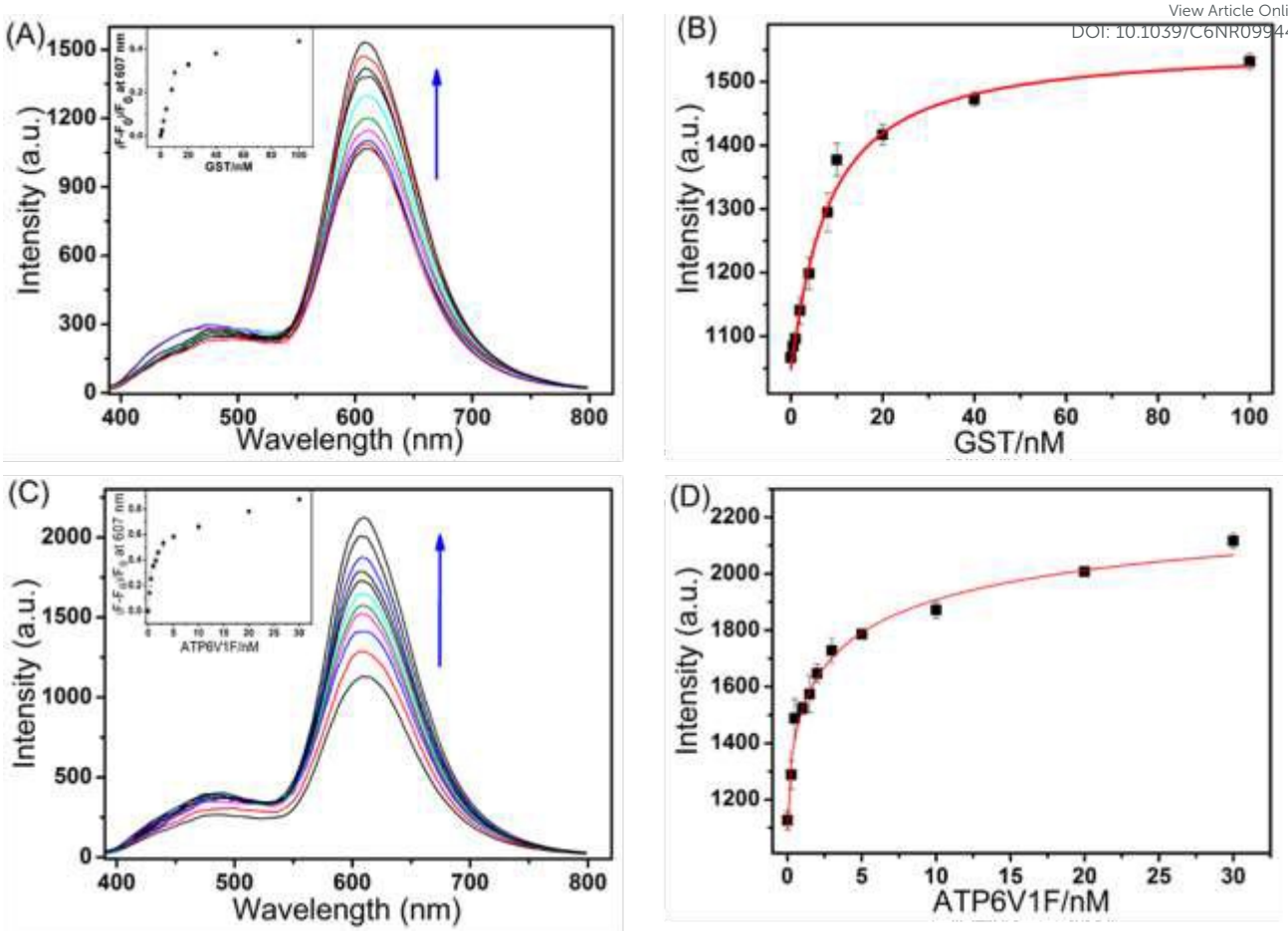

Fig. 5 Fluorescent spectra of the GSH@QDs-GO in the presence of varyious concentrations of GST (0.0, 0.50, 1.0, 2.0, 4.0, 8.0, 10.0, 20.0, 40.0 and 100.0 nM) (A) and ATP6V1F (0.0, 0.25, 0.50, 1.0, 1.5, 2.0, 3.0, 5.0, 10.0, 20.0, and 30.0 nM) (C) (Inset: the fluorescence at 607 nm of QDs@GSH-GO system as a function of the GSTs concentration.). (B, D) Binding constants of QDs@GSH-GO and GSTs were fitted according to the Hill equation. The error bars represented the standard deviations of three independent experiments.

Supplementary Information), and thus an incubation time of 60 min was also used in the subsequent experiments.

Fluorescence detection of GSTs based on QDs@GSH-GO FRET system

To investigate the interaction between QDs@GSH-GO and GSTs, GST and ATP6V1F (a GST tagged protein) as the model analytes were introduced in the experiments. The effect of different concentrations of GSTs on the fluorescence of QDs@GSH was assessed. The fluorescence emissions of the QDs@GSH in presence of GSTs (GST and ATP6V1F) are shown in Fig. 4 (A, B). It is observed that the fluorescence inte-nsity of QDs@GSH decreased along with the incremental amount of GSTs because of the specific interaction between GSH on the surface of QDs and GSTs. The results also revealed that not only the GSH had been successfully modified on the QDs surface, but also this proposed strategy based upon measuring the fluorescence quenching of QDs@GSH was highly sensitive for GSTs determination.[17,22] However, it is not favorable for the application of live cell target imaging due to its turn-off fluorescence. Therefore, a fluorescence turn-on sensor for GSTs detection based on the QDs@GSH-GO FRET system was described. As shown in Fig. 5A, 5C, the quenched fluorescence of QDs@GSH adsorbed on the surface of GO was recovered gradually upon addition of different concentrations of GSTs to the QDs@GSH-GO system. It is suggested that the GSH-GST specific combination is much stronger than the hydrogen bonding interaction between GSH and GO, and the FRET process from QDs@GSH to GO is blocked due to the increasing distance between the energy donor and acceptor.[38] Fig. 5A displayed the relationship between the fluorescence intensity and GST concentration from 0.0 nM (control) to 100.0 nM. It is observed that the fluorescence intensity increased gradually as the concentrations of GST increase. When the concentration of GST was up to 100.0 nM, the fluorescent intensity reached the peak with an increase by about 0.45-fold within 12 min (Fig. S4A, Electronic Supplementary Information). The results exhibited a good linear relationship in the range of 0.0 to 10.0 nM. for GST (Fig. S5A, Electronic Supplementary Information). The detection limit was estimated to be 2.1×10^{-10} M according to 3σ criteria of IUPAC ($3\sigma/m$, σ = 2.12, m = 30.6, Fig. S5C, Electronic Supplementary Information). To our knowledge, the detection limit in this

View Article Online
DOI: 10.1039/C6NR09944K

work is 7 to 4200 times lower than those of fluorescent probes (Table 1). The reason is that the GST leads to the fluorescence recovery of high FRET efficiency from QDs@GSH to GO due to the specific interaction of GST-GSH complexes. The binding constant between QDs@GSH-GO and GST was calculated with

Table 1 Comparison of the proposed method with some other reported methods for determination of GST.

Method	Detection limit (nM)	[Refs.]
Au@GSH NCs	250	[21]
AuNCs@GSH-AuNRs	1.5	[25]
MnO_2-modified UCNPs	900	[55]
C-dot-MnO_2 composite	22	[56]
QDs@GSH-GO	0.21	This work

the Hill equation as follows:

$$F = F_0 + \frac{F_{max} - F_0}{K^n + C^n} \quad (2)$$

Where K is the dissociation constant, C is the concentration of GST in QDs@GSH-GO solution, n is Hill slope, F and F_0 are the fluorescent intensity of QDs@GSH-GO composites in the presence and absence of GST, and F_{max} is the maximum value of fluorescence intensity. The measured K value was 8.0 nM (R^2 = 0.99, n = 1.09). Similarly, the fluorescence emission of QDs@GSH-GO increased by about 0.87-fold in presence of ATP6V1F from 0.0 nM to 10.0 nM shown in Fig. 5C, the combination was completed in presence of 1.0 nM ATP6V1F with 20 min (Fig. S4B, Electronic Supplementary Information), the linear range of ATP6V1F determination was 0.5-3.0 nM (Fig. S5B, Electronic Supplementary Information), the limit of detection of ATP6V1F was estimated to 7.2×10^{-11} M ($3\sigma/m$, σ = 2.12, m = 88.5, Fig. S5D, Electronic Supplementary Information), and the dissociation constant (k) between QDs@GSH-GO and ATP6V1F was measured to be 3.5 nM (R^2 = 0.99, n = 0.58). The overall results demonstrated that the experimental binding strength between FRET system and GSTs in this work was stronger than that in the previous report for the

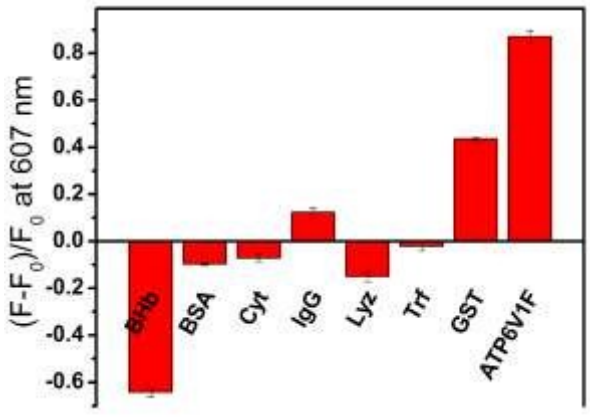

Fig. 6 Fluorescent intensity of the QDs@GSH-GO FRET-based sensor toward GSTs and some other proteins in 10 mM PBS (pH = 7.4). The concentrations of GST, ATP6V1F, BSA, Cyt, BHb, IgG, Lyz and Trf were all 1.0 μM. The concentrations of GST, ATP6V1F, QDs@GSH and GO were 10 nM, 100 nM, 50 mg L^{-1} and 0.24 mg mL^{-1}, respectively. The error bars represented standard deviation of three repetitive experiments.

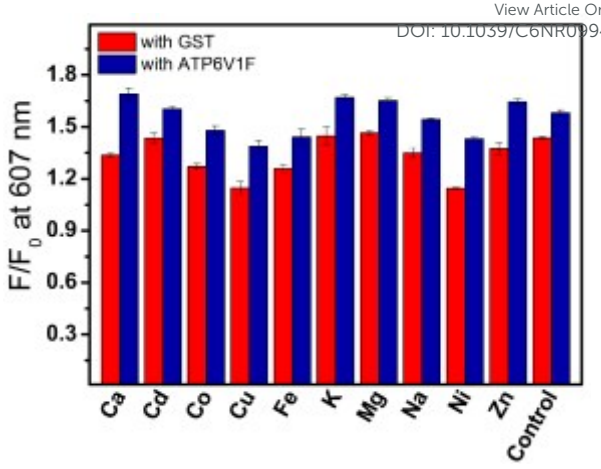

Fig. 7 Fluorescence response of GST or ATP6V1F based on the QDs@GSH-GO in the presence of various metal ions (Ca^{2+}, Cd^{2+}, Co^{2+}, Cu^{2+}, Fe^{3+}, K^+, Mg^{2+}, Na^+, Ni^{2+}, Zn^{2+}). The concentration of each of metal ions is 1 μM. F_0 is the fluorescence intensity of the QDs@GSH-GO system. The error bars represented standard deviation of three repetitive experiments.

GSTs (> 10 nM),[23] and have a lower limit of detection. Therefore, it has been proven that this FRET system have a great potential for the application of GSTs detection in complex samples and in live cell imaging. However, it is not negligible that the fluorescence recovery of the QDs@GSH-GO system is not sufficient with the accumulated concentration of GSTs. As a result, the fluorescence emission signal of the QDs@GSH is still quenched by the high concentration of the GSTs even though the fluorescence emission of the QDs is enhanced by the blocked FRET process.

Selectivity is a key parameter to evaluate the performance of a fluorescent sensing. To identify the selectivity of the FRET system for the GSTs detection, some other proteins such as BHb (pI 6.7), BSA (pI 4.9), Cyt (pI 10.2), IgG (pI 8.0), Lyz (pI 11.0) and Trf (pI 5.6) acted as contrast proteins, the fluorescent response of QDs@GSH-GO to GSTs were carried out in 10 mM PBS (pH = 7.4). As shown in Fig. 6, the QDs@GSH-GO in presence of 100.0 nM for GST and 10.0 nM for ATP6V1F exhibited obvious fluorescence increase by about 0.45-fold and 0.85-fold, respectively. However, the fluo rescence intensity decreased after adding 1.0 μM other proteins to QDs@GSH-GO FRET system except that IgG triggered a slight fluorescence enhancement. Besides, the anti-interference ability of QDs@GSH-GO FRET system to GSTs was also assessed in presence of some metal ions (Ca^{2+}, Cd^{2+}, Co^{2+}, Cu^{2+}, Fe^{3+}, K^+, Mg^{2+}, Na^+, Ni^{2+}, Zn^{2+}). As shown in Fig. 7, 1.0 μM coexisting metal ions had no obvious influence on this approach for GSTs determining, where the Cu^{2+} and Ni^{2+} may coordinate GSH well on the QDs@GSH surface, but resulted in the tiny fluorescence decreasing. Hence, it demonstrated that the QDs@GSH-GO FRET system had a high specificity to GSTs and had a potential for applications *in vivo* and *in vitro* GSTs sensing studies.

QDs@GSH-GO sensing system for detection of GSTs in live cells and urine samples

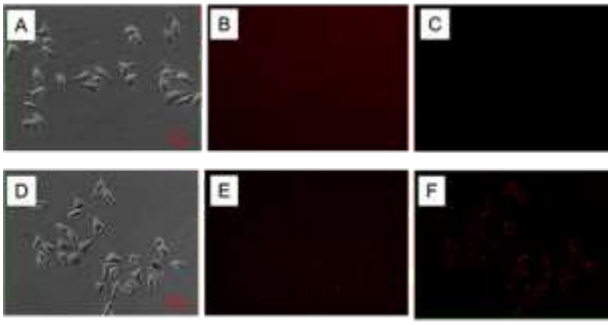

Fig. 8 L929 cells were treated with QDs@GSH-GO. Top panels: (A) L929 cells incubated with QDs@GSH-GO in absence of ATP6V1F in PBS buffer for 30 min at 37 °C shown in bright-field channel; (B) fluorescent image; (C) the overlay image of (A) and (B). Bottom panels: (D) L929 cells incubated with QDs@GSH-GO in presence of 1.0 nM (final concentration) ATP6V1F in PBS buffer for 30 min at 37 °C shown in bright-field channel; (E) fluorescent image; (F) the overlay image of (D) and (E).

To further demonstrate the potential application of QDs@GSH-GO in biological systems, fluorescence imaging experiments of QDs@GSH-GO in living cells were conducted. The L929 cells were incubated with the mixture of QDs@GSH-GO in the absence of ATP6V1F (control) and in the presence of 1.0 nM (final concentration) ATP6V1F for 30 min. The cellular imaging was performed on the inversion fluorescence microscope (Fig. 8). As shown in Fig. 8C, there was not any fluorescence of QDs@GSH-GO in the L929 cells observed from overlay image of bright-field (Fig. 8A) and fluorescence (Fig. 8B) in the control cell lines. In contrast, a relatively bright fluorescence signal appeared in Fig. 8F, the overlay image of bright-field (Fig. 8D) and fluorescence (Fig. 8E). The results exhibited that the concentration of ATP6V1F lower down to 1.0 nM in live cells could generate a strong intracellular fluorescence recovery of QDs@GSH-GO. The results indicate that the QDs@GSH-GO FRET system can be applied to sense the intracellular GSTs in living cells possessing low toxicity and good biocompatibility.

Table 2 Recovery (mean±s; n=3) for GSTs detection in urine sample

Sample	GSTs added (nM)	GSTs found (nM)	Recovery (%)
urine 1	0.5	0.4 ± 0.04	80.0 ± 8.0
urine 2	1.0	0.9 ± 0.05	90.0 ± 5.0

The QDs@GSH-GO system was also applied to monitor the GSTs in human urine samples. It was reported that elevated levels of specific GSTs have been detected in several kidney-related diseases.[54] As a result, ATP6V1F, as the model of the GSTs, was spiked to the urine sample diluted by 100-fold with QDs@GSH-GO system (Fig. S6, Electronic Supplementary Information). The concentrations of spiked ATP6V1F 0.5 and 1.0 nM (final concentration) were monitored by QDs@GSH-GO, and the recovery is 80.0%-90.0% (Table 2). The results suggested that this sensor has great potential for determining the GSTs concentration in complex biological samples.

Conclusions

In summary, on the basis of the specific interaction between GSH and GSTs, we have fabricated a novel fluorescent sensor for GSTs detection based on QDs@GSH-GO FRET system. This fluorescence sensor shows high selectivity and sensitivity, great binding constants and low limit of detection for GST and the GST-tagged protein. Moreover, the proposed approach has been successfully applied for the assay of GSTs in complex biological samples and live cell imaging with minimal background interference even at low concentrations of analytes. It is expected that the Mn-doped ZnS QDs-GO will provide new opportunities for ratiometric, nontoxic, sensitive chemo/bio-detection in biomedical area.

Acknowledgements

This work was supported by the National Natural Science Foundation of China (No. 21475067, 21275080), and the Natural Science Foundation of Tianjin (No. 15JCYBJC20600).

Notes and references

1 H. Dirr, P. Reinemer and R. Huber, *Eur. J. Biochem.*, 1994, **220**, 645-661.
2 M. C. Wilce and M. W. Parker, *Biochim. Biophys. Acta*., 1994, **1205**, 1-18.
3 P. G. Board and M. W. Anders, *Chem. Res. Toxicol.*, 2007, **20**, 149-154.
4 S. Singh, *Cancer Chemother Pharmacol.*, 2015, **75**, 1-15.
5 G. Di Pietro, L. A. Magno and F. Rios-Santos, *Expert Opin. Drug Metab. Toxicol*., 2010, **6**, 153-170.
6 M. W. Van Gisbergen, M. Cebula, J. Zhang, A. Ottosson-Wadlund, L. Dubois, P. Lambin, K. D. Tew, D. M. Townsend, G. R. M. M. Haenen, M. J. D. R. Drittij-Reijnders, H. Saneyoshi, M. Araki, Y. Shishido, Y. Ito, E. S. J. Arner, H. Abe, R. Morgenstern, and K. Johansson, *Mol. Pharmaceutics*., 2016, **13**, 2010-2025.
7 J. V. Frangioni and B. G. Neel, *Anal. Biochem.*, 1993, **210**, 179-187.
8 C. M. Kolodziej, C. W. Changx and H. D. Maynard, *J. Mater. Chem.*, 2011, **21**, 1457-1461.
9 R. M. Katusz, B. Bono and R. F. Colman, *Biochemistry*, 1992, **31**, 8984-8990.
10 N. E. Pettigrew, E. J. Brush and R. F. Colman, *Biochemistry*, 2001, **40**, 7549-7558.
11 W. J. Lo, Y. C. Chiou, Y. T. Hsu, W. S. Lam, M. Y. Chang, S. C. Jao and W. S. Li, *Bioconjugate Chem.*, 2007, **18**, 109-120.
12 W. D. Lu and W. M. Atkins, *Biochemistry*, 2004, **43**, 12761-12769.
13 W. B. Anderson, D. C. Liebler, P. G. Board and M. W. Anders, *Chem. Res. Toxicol*., 2002, **15**, 1387-1397.
14 E. W. Lin, N. Boehnke and H. D. Maynard, *Bioconjugate Chem.*, 2014, **25**, 1902-1909.
15 M. C. Martos-Maldonado, I. Quesada-Soriano, F. García-Maroto, A. Vargas-Berenguel and L. García-Fuentes, *Bioorg. Med. Chem. Lett.*, 2012, **22**, 7256-7260.
16 W. H. Zhou, J. W. Shultz, N. Murphy, E. M. Hawkins, L. Bernad, T. Good, L. Moothart, S. Frackman, D. H. Klaubert, R. F. Bulleitb and K. V. Wood, *Chem. Commun.*, 2006, 4620-4622.
17 M. Hasegawa, Y. Tsukasaki, T. Ohyanagia and T. Jin, *Chem. Commun.*, 2013, **49**, 228-230.
18 Y. Pan, M. J. C. Long, X. M. Li, J. F. Shi, L. Hedstrom and B. Xu, *Chem. Sci.*, 2011, **2**, 945-948.
19 M. W. Ayad and D. A. Nafea, *Comp. Clin. Pathol.*, 2014, **23**, 1023-1029.
20 D. D. Zheng, D. Pan, X. Zha, Y. Q. Wu, C. L. Jiang and X. H. Yu, *Chem. Commun.*, 2013, **49**, 8546-8548.

View Article Online
DOI: 10.1039/C6NR09944K

21 C. T. Chen, W. J. Chen, C. Z. Liu, L. Y. Chang and Y. C. Chen, *Chem. Commun.*, 2009, 7515-7517.
22 J. J. Beato-López, C. Fernández-Ponce, E. Blanco and R. C. M. Barrera-Solano, *Nanomater. Nanotechnol.*, 2012, **2**, 1-9.
23 L. Unger-Angel, B. Rout, T. Ilani, M. Eisenstein and D. Margulies, *Chem. Sci.*, 2015, **6**, 5419-5425.
24 J. Zhang, A. Shibata, M. Ito, S. Shuto, Y. Ito, B. Mannervik, H. Abe and R. Morgenstern, *J. Am. Chem. Soc.*, 2011, **133**, 14109-14119.
25 L. Qin, X. W. He, L. X. Chen and Y. K. Zhang, *ACS Appl. Mater. Interfaces*, 2015, **7**, 5965-5971.
26 Y. Pan, A. Leifert, D. Ruau, S. Neuss, J. Bornemann, G. Schmid, W. Brandau, U. Simon and W. Jahnen-Dechent, *Small*, 2009, **5**, 2067-2076.
27 B. Y. Wu, H. F. Wang, J. T. Chen and X. P. Yan, *J. Am. Chem. Soc.*, 2011, **133**, 686-688.
28 S. J. Wu, N. Duan, X. Y. Ma, Y. Xia, Y. Yu, Z. P. Wang and H. X. Wang, *Chem. Commun.*, 2012, **48**, 4866-4868.
29 L. Wu, Q. S. Guo, Y. Q. Liu and Q. J. Sun, *Anal. Chem.*, 2015, **87**, 5318-5323.
30 S. J. Wu, N. Duan, X. Y. Ma, Y. Xia, H. X. Wang, Z. P. Wang and Q. Zhang, *Anal. Chem.*, 2012, **84**, 6263-6270.
31 R. Kikkeri, V. Padler-Karavani, S. Diaz, A. Verhagen, H. Yu, H. Z. Cao, M. A. Langereis, R. J. De Groot, X. Chen and A. Varki, *Anal. Chem.*, 2013, **85**, 3864-3870.
32 E. Oh, D. Lee, Y. P. Kim, S. Y. Cha, D. B. Oh, H. A. Kang, J. Kim, and H. S. Kim, *Angew. Chem. Int. Ed.*, 2006, **45**, 7959-7963.
33 X. Gao, D. Li, Y. Tong, D. Ge, Y. W. Tang, D. F. Zhang and J. R. Li, *Luminescence*, 2015, **30**, 1389-1394.
34 P. Zhang, S. Rogelj, K. Nguyen and D. Wheeler, *J. Am. Chem. Soc.*, 2006, **128**, 12410-12411.
35 L. F. Shi, V. D. Paoli, N. Rosenzweig and Z. Rosenzweig, *J. Am. Chem. Soc.*, 2006, **128**, 10378-10379.
36 L. F. Shi, N. Rosenzweig and Z. Rosenzweig, *Anal. Chem.*, 2007, **79**, 208-214.
37 E. Oh, M. Y. Hong, D. Lee, S. H. Nam, H. C. Yoon and H. S. Kim, *J. Am. Chem. Soc.*, 2005, **127**, 3270-3271.
38 Y. M. Wu, Y. Cen, L. J. Huang, R. Q. Yu and X. Chu, *Chem. Commun.*, 2014, **50**, 4759-4762.
39 J. R. Kyle, C. S. Ozkan and M. Ozkan, *Nanoscale*, 2012, **4**, 3807-819.
40 J. K. Yang, S. Y. Kwak, S. J. Jeon, E. Lee, J. M. Ju, H. I. Kim, Y. S. Lee and J. H. Kim, *Nanoscale*, 2016, **8**, 12272–12281.
41 J. J. Liu, X. R. Song, Y. W. Wang, G. N. Chen and H. H. Yang. *Nanoscale*, 2012, **4**, 3655-3659.
42 H. F. Dong, W. C. Gao, F. Yan, H. X. Ji and H. X. Ju, *Anal. Chem.*, 2010, **82**, 5511-5517.
43 R. S. Swathi and K. L. Sebastiana, *J. Chem. Phys.*, 2008, **129**, 054703.
44 R. S. Swathi and K. L. Sebastiana, *J. Chem. Phys.*, 2009, **130**, 086101.
45 F. M. Winnik and D. Maysinger, *Acc. Chem. Res.*, 2013, **46**, 672-680.
46 P. Wu and X. P. Yan, *Chem. Soc. Rev.*, 2013, **42**, 5489-5521.
47 R. Thaker, Y. C. Chen and P. T. Snee, *Nano Lett.*, 2007, **7**, 3429-3432.
48 S. M. Emin, N. Sogoshi, S. Nakabayashi, T. Fujihara and C. D. Dushkin, *J. Phys. Chem. C*, 2009, **113**, 3998-4007.
49 S. Sarkar, R. Bose, S. Jana, N. R. Jana and N. Pradhan, *J. Phys. Chem. Lett.*, 2010, **1**, 636-640.
50 G. Mayer and A. Heckel, *Angew. Chem. Int. Ed.*, 2006, **45**, 4562-4589.
51 D. Zhu, X. X. Jiang, C. Zhao, X. L. Sun, J. R. Zhang and J. J. Zhu, *Chem. Commun.*, 2010, **46**, 5226-5228.
52 N. S. Karan, D. D. Sarma, R. M. Kadam and N. Pradhan, *J. Phys. Chem. Lett.*, 2010, **1**, 2863-2866.
53 H. F. Wang, Y. He, T. R. Ji and X. P. Yan, *Anal. Chem.*, 2009, **81**, 1615-1621.
54 T. J. Cawood, M. Bashir, J. Brady, B. Murray, P. T. Murray and D. O'Shea, *Am. J. Nephrol.*, 2010, **32**, 219-225.
55 R. R. Deng, X. J. Xie, M. Vendrell, Y. T. Chang and X. G. Liu, *J. Am. Chem. Soc.*, 2011, **133**, 20168-20171.
56 Y. H. Wang, K. Jiang, J. L. Zhu, L. Zhang and H. W. Liu, *Chem. Commun.*, 2015, **51**, 12748-12751.